Belle Preprint 2002-25

KEK Preprint 2002-72

Observation of $B \to D^{(*)} K^- K^{0(*)}$ decays

Belle Collaboration

A. Drutskoy [k], K. Abe [g], K. Abe [an], N. Abe [aq], R. Abe [ab], T. Abe [ao], I. Adachi [g], Byoung Sup Ahn [n], H. Aihara [ap], M. Akatsu [u], Y. Asano [au], T. Aso [at], V. Aulchenko [a], T. Aushev [k], A. M. Bakich [ak], Y. Ban [af], E. Banas [z], A. Bay [q], I. Bedny [a], P. K. Behera [av], I. Bizjak [ℓ], A. Bondar [a], A. Bozek [z], T. E. Browder [f], B. C. K. Casey [f], M.-C. Chang [y], P. Chang [y], Y. Chao [y], K.-F. Chen [y], B. G. Cheon [aj], R. Chistov [k], S.-K. Choi [e], Y. Choi [aj], Y. K. Choi [aj], M. Danilov [k], L. Y. Dong [i], S. Eidelman [a], V. Eiges [k], Y. Enari [u], C. W. Everton [t], F. Fang [f], C. Fukunaga [ar], N. Gabyshev [g], A. Garmash [a,g], T. Gershon [g], R. Guo [w], J. Haba [g], T. Hara [ad], Y. Harada [ab], H. Hayashii [v], M. Hazumi [g], E. M. Heenan [t], I. Higuchi [ao], T. Higuchi [ap], L. Hinz [q], T. Hokuue [u], Y. Hoshi [an], W.-S. Hou [y], S.-C. Hsu [y], H.-C. Huang [y], T. Igaki [u], Y. Igarashi [g], T. Iijima [u], K. Inami [u], A. Ishikawa [u], H. Ishino [aq], R. Itoh [g], H. Iwasaki [g], Y. Iwasaki [g], H. K. Jang [ai], J. H. Kang [ay], J. S. Kang [n], P. Kapusta [z], S. U. Kataoka [v], N. Katayama [g], H. Kawai [b], Y. Kawakami [u], T. Kawasaki [ab], H. Kichimi [g], D. W. Kim [aj], Heejong Kim [ay], H. J. Kim [ay], Hyunwoo Kim [n], T. H. Kim [ay], K. Kinoshita [d], S. Korpar [s,ℓ], P. Križan [r,ℓ], P. Krokovny [a], R. Kulasiri [d], S. Kumar [ae], A. Kuzmin [a],

Y.-J. Kwon [ay], G. Leder [j], S. H. Lee [ai], J. Li [ah], D. Liventsev [k], R.-S. Lu [y], J. MacNaughton [j], G. Majumder [aℓ], F. Mandl [j], D. Marlow [ag], T. Matsuishi [u], S. Matsumoto [c], T. Matsumoto [ar], W. Mitaroff [j], Y. Miyabayashi [u], H. Miyake [ad], H. Miyata [ab], G. R. Moloney [t], T. Mori [c], T. Nagamine [ao], Y. Nagasaka [h], T. Nakadaira [ap], E. Nakano [ac], M. Nakao [g], J. W. Nam [aj], Z. Natkaniec [z], K. Neichi [an], S. Nishida [o], O. Nitoh [as], S. Noguchi [v], T. Nozaki [g], S. Ogawa [am], F. Ohno [aq], T. Ohshima [u], T. Okabe [u], S. Okuno [m], S. L. Olsen [f], Y. Onuki [ab], W. Ostrowicz [z], H. Ozaki [g], P. Pakhlov [k], H. Palka [z], C. W. Park [n], H. Park [p], L. S. Peak [ak], J.-P. Perroud [q], M. Peters [f], L. E. Piilonen [aw], N. Root [a], M. Rozanska [z], K. Rybicki [z], H. Sagawa [g], S. Saitoh [g], Y. Sakai [g], H. Sakamoto [o], M. Satapathy [av], A. Satpathy [g,d], O. Schneider [q], S. Schrenk [d], S. Semenov [k], K. Senyo [u], R. Seuster [f], M. E. Sevior [t], H. Shibuya [am], V. Sidorov [a], J. B. Singh [ae], N. Soni [ae], S. Stanič [au,1], M. Starič [ℓ], A. Sugi [u], A. Sugiyama [u], K. Sumisawa [g], T. Sumiyoshi [ar], S. Y. Suzuki [g], T. Takahashi [ac], F. Takasaki [g], K. Tamai [g], N. Tamura [ab], J. Tanaka [ap], M. Tanaka [g], G. N. Taylor [t], Y. Teramoto [ac], S. Tokuda [u], M. Tomoto [g], T. Tomura [ap], S. N. Tovey [t], K. Trabelsi [f], T. Tsuboyama [g], T. Tsukamoto [g], S. Uehara [g], K. Ueno [y], Y. Unno [b], S. Uno [g], Y. Ushiroda [g], G. Varner [f], K. E. Varvell [ak], C. C. Wang [y], C. H. Wang [x], J. G. Wang [aw], M.-Z. Wang [y], Y. Watanabe [aq], E. Won [n], B. D. Yabsley [aw], Y. Yamada [g], A. Yamaguchi [ao], Y. Yamashita [aa], M. Yamauchi [g], H. Yanai [ab], P. Yeh [y], Y. Yusa [ao], J. Zhang [au], Z. P. Zhang [ah], V. Zhilich [a], and D. Žontar [au]

[a] *Budker Institute of Nuclear Physics, Novosibirsk, Russia*

[b] *Chiba University, Chiba, Japan*

[c] *Chuo University, Tokyo, Japan*

[d] *University of Cincinnati, Cincinnati, OH, USA*

[e] *Gyeongsang National University, Chinju, South Korea*

[f] *University of Hawaii, Honolulu, HI, USA*

[g] *High Energy Accelerator Research Organization (KEK), Tsukuba, Japan*

[h] *Hiroshima Institute of Technology, Hiroshima, Japan*

[i] *Institute of High Energy Physics, Chinese Academy of Sciences, Beijing, PR China*

[j] *Institute of High Energy Physics, Vienna, Austria*

[k] *Institute for Theoretical and Experimental Physics, Moscow, Russia*

[ℓ] *J. Stefan Institute, Ljubljana, Slovenia*

[m] *Kanagawa University, Yokohama, Japan*

[n] *Korea University, Seoul, South Korea*

[o] *Kyoto University, Kyoto, Japan*

[p] *Kyungpook National University, Taegu, South Korea*

[q] *Institut de Physique des Hautes Énergies, Université de Lausanne, Lausanne, Switzerland*

[r] *University of Ljubljana, Ljubljana, Slovenia*

[s] *University of Maribor, Maribor, Slovenia*

[t] *University of Melbourne, Victoria, Australia*

[u] *Nagoya University, Nagoya, Japan*

[v] *Nara Women's University, Nara, Japan*

[w] *National Kaohsiung Normal University, Kaohsiung, Taiwan*

[x] *National Lien-Ho Institute of Technology, Miao Li, Taiwan*

[y] *National Taiwan University, Taipei, Taiwan*

[z] *H. Niewodniczanski Institute of Nuclear Physics, Krakow, Poland*

[aa] *Nihon Dental College, Niigata, Japan*

[ab] *Niigata University, Niigata, Japan*

[ac] *Osaka City University, Osaka, Japan*

[ad] *Osaka University, Osaka, Japan*

[ae] *Panjab University, Chandigarh, India*

[af] *Peking University, Beijing, PR China*

[ag] *Princeton University, Princeton, NJ, USA*

[ah] *University of Science and Technology of China, Hefei, PR China*

[ai] *Seoul National University, Seoul, South Korea*

[aj] *Sungkyunkwan University, Suwon, South Korea*

[ak] *University of Sydney, Sydney, NSW, Australia*

[aℓ] *Tata Institute of Fundamental Research, Bombay, India*

[am] *Toho University, Funabashi, Japan*

[an] *Tohoku Gakuin University, Tagajo, Japan*

[ao] *Tohoku University, Sendai, Japan*

[ap] *University of Tokyo, Tokyo, Japan*

[aq] *Tokyo Institute of Technology, Tokyo, Japan*
[ar] *Tokyo Metropolitan University, Tokyo, Japan*
[as] *Tokyo University of Agriculture and Technology, Tokyo, Japan*
[at] *Toyama National College of Maritime Technology, Toyama, Japan*
[au] *University of Tsukuba, Tsukuba, Japan*
[av] *Utkal University, Bhubaneswer, India*
[aw] *Virginia Polytechnic Institute and State University, Blacksburg, VA, USA*
[ay] *Yonsei University, Seoul, South Korea*

Abstract

The $B \to D^{(*)}K^-K^{(*)0}$ decays have been observed for the first time. The branching fractions of the $B \to D^{(*)}K^-K^{(*)0}$ decay modes are measured. Significant signals are found for the $B \to D^{(*)}K^-K^{*0}$ and $B^- \to D^0K^-K^0_S$ decay modes. The invariant mass and polarization distributions for the K^-K^{*0} and $K^-K^0_S$ subsystems have been studied. For the K^-K^{*0} sybsystem these distributions agree well with those expected for two-body $B \to D^{(*)}a_1^-(1260)$ decays, with $a_1^-(1260) \to K^-K^{*0}$. The analysis was done using 29.4 fb^{-1} of data collected with the Belle detector at the e^+e^- asymmetric collider KEKB.

Key words: B decay, branching fraction, $s\bar{s}$ pair
PACS: 13.25.Hw, 14.40.Cs, 14.40.Nd

[1] on leave from Nova Gorica Polytechnic, Nova Gorica, Slovenia

1 Introduction

In this paper we report on the first observation of B meson decays to $D^{(*)}K^-K^{(*)0}$ final states [1]. Such decays require the creation of an additional $s\bar{s}$ pair and can occur via the quasi-two-body mechanism shown in Fig. 1a, where the intermediate resonance decays to $K^-K^{0(*)}$, or by a non-resonant three-body decay shown in Fig. 1b. Contributions from color-suppressed diagrams are expected to be small [1]. The investigation of these processes can provide important information for testing various models of hadronic B decays as well as for studies of $K^-K^{0(*)}$ resonant states.

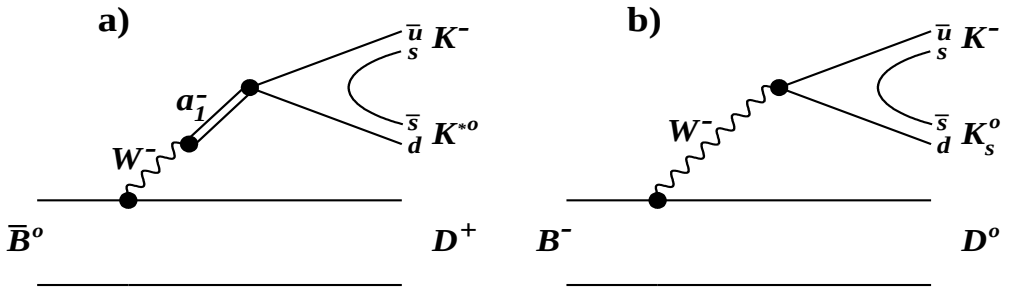

Fig. 1. The external spectator diagrams for a) quasi-two-body and b) non-resonant three-body B meson decays with the $s\bar{s}$ pair creation. The decay channels $\bar{B^0} \to D^+K^-K^{*0}$ and $B^- \to D^0K^-K_S^0$ are used as examples.

In $B \to D^{(*)}K^-K^{(*)0}$ decays, any intermediate $K^-K^{0(*)}$ resonance must have isospin 1. The allowed quantum numbers are $J^P = 0^-, 1^-, 1^+$ for the K^-K^{*0} final state and $J^P = 1^-$ for the $K^-K_S^0$ final state. A $K^-K_S^0$ state with $J^P = 0^+$ cannot be produced via tree diagrams of Figs. 1a,b [2] in the limit of exact isospin symmetry. The production of resonances with spin larger than one is forbidden in the factorization approach [1]. Furthermore, these restrictions on the quantum numbers for $K^-K^{0(*)}$ resonant states also hold for non-resonant $K^-K^{0(*)}$ production (Fig. 1b) [2].

In the case of decays via intermediate resonances, the final state branching fraction depends on both the production and decay rates of the resonance. Large production rates of the order of 1% have been observed for the $B \to D^{(*)}a_1(1260)$ and $B \to D^{(*)}\rho(770)$ decay channels [3]. The K^-K^{*0} final state can be produced in the decay of the $a_1^-(1260)$ resonance, however, the branching fraction for $a_1^-(1260) \to K^-K^{*0}$, which was indirectly determined in τ decays by the CLEO collaboration [4], was found to be only $(3.3 \pm 0.5)\%$. One also expects that for the $J^P = 1^-$ resonances $\rho(1450)$ and $\rho(1700)$ the branching fractions to $K^-K^{0(*)}$ are at the level of a few percent or less [5].

[1] Charge conjugate modes are implicitly included.

For $K^- K^0_S$ production in $\rho(770)$ meson decay the phase space is very limited.

In contrast to two-body decays, non-resonant three-body B decays to one charmed and two light mesons have not yet been observed [3]. It should be noted that $s\bar{s}$ pair creation in a non-resonant three-body B decay (Fig. 1b) is only moderately suppressed relative to that for $u\bar{u}$ and $d\bar{d}$ pairs if SU(3) and phase space effects are taken into account [6]. Unfortunately, quasi-two-body and three-body processes cannot be easily separated because of the large widths of the intermediate resonances.

The branching fractions for D decays with $s\bar{s}$ creation are measured to be $\sim (1-2)\%$ [5]. However, these values cannot be directly extrapolated to B decay because final state interactions, which are much larger for D decays, can significantly affect the decay rates. A possible similarity between the diagrams of Fig. 1 and those describing τ lepton decays with $K^- K^{0(*)}$ in the final state is obscured by the rather limited phase space, resulting in small branching fractions for τ decays to $K^- K^0 \nu_\tau$ and $K^- K^{*0} \nu_\tau$ when compared to non-$s\bar{s}$ channels.

In this paper the branching fractions for $B \to D^{(*)} K^- K^{(*)0}$ decays are obtained for the full allowed kinematic region. The invariant mass and polarization distributions of the $K^- K^{0(*)}$ subsystem are then studied in detail.

2 Belle Detector

The data were collected with the Belle detector at KEKB, an asymmetric energy double storage ring collider with 8 GeV electrons and 3.5 GeV positrons [7]. The results are based upon a data sample with an integrated luminosity of 29.4 fb^{-1} taken at the $\Upsilon(4S)$ resonance which corresponds to 31.9 million $B\bar{B}$ pairs.

Belle is a general-purpose detector with a 1.5 T superconducting solenoid magnet. Charged particle tracking is provided by a silicon vertex detector (SVD), consisting of three nearly cylindrical layers of double-sided silicon strip detectors, and a 50-layer central drift chamber (CDC). Particle identification is accomplished by combining the information from silica aerogel Čerenkov counters (ACC) and a time-of-flight counter system (TOF) with specific ionization (dE/dx) measurements in the CDC. The combined response of the three systems provides at least 2.5σ equivalent K/π separation for laboratory momenta up to 3.5 GeV/c. A CsI(Tl) electromagnetic calorimeter (ECL) located inside the solenoid coil is used for detection of photons and electrons. The detector is described in detail elsewhere [8].

The Monte Carlo (MC) simulation event samples used in this analysis were generated using a detailed GEANT-based simulation of the Belle detector response. Simulated events were processed in a manner similar to the data.

3 Selection Criteria

The charged track momenta are reconstructed using the CDC and SVD tracking system. Kaon and pion mass hypotheses are assigned to charged tracks using a likelihood ratio $P(K/\pi) = L(K)/(L(K)+L(\pi))$, which ranges between 0 and 1. $P(K/\pi) > 0.6$ is required for kaon candidates and $P(K/\pi) < 0.6$ for pion candidates.

Candidate π^0 mesons are reconstructed from pairs of photons in the ECL with invariant masses within $\pm 15\,\mathrm{MeV/c^2}$ of the nominal π^0 mass ($\sim 3\sigma$ in the π^0 mass resolution). The π^0 daughter photons are required to have energies greater than 30 MeV. A mass-constrained kinematic fit is performed on the π^0 candidates to improve their energy resolution.

K^0_S candidates are formed from $\pi^+\pi^-$ combinations with an invariant mass within $\pm 10\,\mathrm{MeV/c^2}$ of the nominal K^0_S mass ($\sim 3\sigma$). The two pions are required to have a common vertex that is displaced from the interaction point by at least 0.4 cm in the plane perpendicular to the beam direction. The difference in z coordinates (parallel to the beam direction) for the tracks constituting the secondary vertex is required to be less than 2 cm. The angle α between the K^0_S flight direction and the measured K^0_S momentum direction is required to satisfy $\cos\alpha > 0.8$.

An opposite sign K and π meson combination is taken as a K^{*0} candidate if its invariant mass lies within a $\pm 50\,\mathrm{MeV/c^2}$ interval of the nominal K^{*0} mass.

The decay channels $D^+ \to K^-\pi^+\pi^+$ and $D^0 \to K^-\pi^+$ are used in this analysis for all studied B decay modes, in order to avoid large combinatorial background. The decay channel $D^0 \to K^-\pi^-\pi^+\pi^+$ is only added for the D^{*0} and D^{*+} meson reconstruction, because the D^* constraint strongly suppresses the combinatorial background. The invariant mass of the D candidates is required to lie within $\pm 15\,\mathrm{MeV/c^2}$ of the nominal D mass for the first two modes and within $\pm 12\,\mathrm{MeV/c^2}$ for the $K^-\pi^-\pi^+\pi^+$ mode ($\sim 3\sigma$). A mass and vertex constrained kinematic fit is then performed on the D candidates and results of good quality fits are used to improve the D momentum resolution.

For D^{*0} and D^{*+} candidates, the $D^{*0} \to D^0\pi^0$ and $D^{*+} \to D^0\pi^+$ decay modes are used. The invariant mass of the D^0 and π combination is required to be within $\pm 3.0\,\mathrm{MeV/c^2}$ of the nominal value for D^{*0} ($\sim 3\sigma$) and within

± 1.5 MeV/c^2 for D^{*+} ($\sim 3\sigma$).

The D and D^* candidates are combined with the $K^- K^0_S$ and $K^- K^{*0}$ candidates to form B^- and $\bar{B}^0$ candidates. Two kinematic variables are used to extract the B meson signal, the energy difference $\Delta E = E_B^{\rm CM} - E_{\rm beam}^{\rm CM}$ and the beam-constrained mass $M_{\rm bc} = \sqrt{(E_{\rm beam}^{\rm CM})^2 - (p_B^{\rm CM})^2}$, where $E_B^{\rm CM}$ and $p_B^{\rm CM}$ are the center of mass (CM) energy and momentum of the B candidate and $E_{\rm beam}^{\rm CM}$ is the CM beam energy. The intervals $M_{\rm bc} > 5.2\,{\rm GeV/c^2}$ and $|\Delta E| < 0.2\,{\rm GeV}$ are selected. The MC estimate of the $M_{\rm bc}$ resolution is in the range (2.7–3.0) MeV/c^2; the ΔE resolution ranges between 12.5 and 14.5 MeV for final states including π^0's and between 8.5 and 10.5 MeV for other final states. The background from $B \to D^{(*)} D_s^-$ decay modes, with $D_s^- \to K^- K^{0(*)}$, is removed by requiring $|M(D_s^-) - M(K^- K^{0(*)})| > 20\,{\rm MeV/c^2}$ ($\sim 4\sigma$). Only one B meson candidate per event is accepted. In cases of multiple entries, the chosen candidate is the one with the largest likelihood value, which is calculated using information about the differences between nominal and measured D, D^* and π^0 masses and the charged particle identification.

The continuum background under the $\Upsilon(4S)$ signal is suppressed by topological cuts that were optimized using MC to model the signal and data in the B mass sideband ($5.2 < M_{\rm bc} < 5.26$) GeV/c^2 to model background. The ratio of the second to the zeroth Fox-Wolfram moments [9] is required to be less than 0.5. The angle θ^*_{thr} in the CM between the thrust axes of the particles forming the B candidate and all other particles in the event must satisfy $|\cos(\theta^*_{thr})| < 0.85$. The angle θ^*_B in the CM between the beam direction and the B momentum direction should lie in the range $|\cos(\theta^*_B)| < 0.9$.

4 Systematics and Backgrounds

The systematic uncertainties described below were estimated and added in quadrature to obtain final systematic errors separately for each decay channel. The contributions are listed in Table 1.

A significant systematic uncertainty comes from the uncertainty of the charged track reconstruction efficiency, which has been evaluated from data. This uncertainty is estimated to be 2% per track for tracks with momentum larger than 200 MeV/c. A special study was performed to determine the momentum dependence of the reconstruction efficiency of the charged low momentum pion ($P^{CM}(\pi_{slow}) < (220 - 250)$MeV/c) from the D^{*+} meson decay. The distribution of the helicity angle, which is strongly correlated with the slow pion momentum, is compared in MC and data for $B^0 \to D^{*+}\pi^-$ decays. Good agreement of the shapes of these distributions is obtained. A similar method is used to estimate the reconstruction efficiency of a π^0 meson produced in D^{*0}

decay. A test of the relative reconstruction efficiencies for low momentum π^+ and π^0 was performed by comparing two inclusive D^{*+} decay modes. The ratio of the branching fractions $R_{D^{*+}} = Br(D^{*+} \to D^+\pi^0)/Br(D^{*+} \to D^0\pi^+)$ was determined in generic $B\bar{B}$ MC and data. Reasonable agreement was obtained. A 10% systematic uncertainty is added to take into account the uncertainty in the reconstruction efficiency for both charged and neutral slow pions.

The charged kaon and pion identification efficiency is checked by fitting the $D^{*+} \to D^0\pi^+$, $D^0 \to K^-\pi^+$ signal in MC and data. The fractions of signal events with and without kaon or pion identification are compared in the D^{*+} center-of-mass momentum range from 1.0 to 2.5 GeV/c. This systematic error is found to be around 1% per particle. A similar procedure is applied to check the K^0_S selection efficiency, where the $D^{*+} \to D^0\pi^+$, $D^0 \to K^0_S\pi^+\pi^-$ decay channel is used. The systematic uncertainty obtained is 3%.

The non-resonant background under the K^{*0} signal is estimated from a fit using a relativistic Breit-Wigner function for the signal and a linear function to describe the non-resonant background. The mass and width of the K^{*0} are in good agreement with the nominal values. The non-resonant contribution under the K^{*0} is found to be $(2 \pm 2)\,\%$. No correction is applied and an uncertainty of 4% was added for this background source. The efficiency of the D meson mass and vertex constrained kinematic fit is close to 100% with about a 1% uncertainty. The uncertainties in the D and D^* meson decay branching fractions were also taken into account [5].

The probability of finding more than one B candidate per event is generally not large and is well reproduced by MC. The fraction of multiple entries varies from 2% for channels with only charged tracks in the final state, to 17% for channels with a D^{*0}. The uncertainty in the signal yield due to this effect is estimated to be 4% for the decay modes with a D^{*0} and 2% for other decay modes.

The background under the B signal is separated into the combinatorial background, which is removed by the fit procedure, and peaking backgrounds, where the content of the final particles is the same as in the studied channel, but a D meson was not formed. The systematic uncertainty of the combinatorial background subtraction is estimated by varying the function that describes the background shape. This uncertainty is smaller than 5%. The width of the signal Gaussian is also varied inside the acceptable range and this systematic error is found to be in the range (3–5)%. The uncertainty in the estimate of the peaking background is found to be approximately 5% for the $B^- \to D^0K^-K^0_S$ and $B^- \to D^0K^-K^{*0}$ decay channels and significantly smaller for other channels, if this background is evaluated from D meson sideband studies.

The MC distributions of K^-K^{*0} and $K^-K^0_S$ mass were adjusted to describe

the data. The shapes of these distributions are varied within their experimental uncertainties. For modes with D^{*0} and D^{*+} mesons the polarization is varied from longitudinal to transverse. The uncertainty in the determination of the number of $B\bar{B}$ pairs for the full data sample is 1%. Finally, the MC statistical uncertainties are also included in the systematic uncertainty. The overall systematic uncertainty ranges from 15 to 19% for modes with D mesons and from 19 to 22% for modes with D^* mesons (Table 1).

Table 1
The systematic uncertainties in the branching fraction calculations.

1.	Reconstruction efficiency	
	a) Charged track (per track)	2%
	b) Slow π^+ from D^{*+}	10%
	c) Slow π^0 from D^{*0}	10%
	d) K^0_s, K^{*0}, D^0 and D^+ mesons	(1-3)%
2.	$\pi^\pm/K^\pm$ identification (per particle)	1%
3.	Background subtraction	
	a) Combinatorial background shape	(1-5)%
	b) B signal width	(3-5)%
	c) Combinatorial background under D^0	(1-5)%
	d) Non-resonant background under K^{*0}	4%
4.	MC model	
	a) D^{*0} and D^{*+} polarization	(4-8)%
	b) $K^-K^{0(*)}$ mass shape	(2-3)%
	c) B candidate multiple entries	(2-4)%
	d) MC statistical error	(3-6)%
5.	D and D^* branching fractions	(2-7)%
6.	Number of B mesons	1%
	Total: D modes	$\sim (15-19)\%$
	Total: D^* modes	$\sim (19-22)\%$

5 Results

After applying all the selection requirements, the signal yields for the eight decay channels are obtained from fits to the ΔE distributions shown in Fig. 2. Because the ΔE and $M_{\rm bc}$ parameters are almost independent, an additional selection $M_{\rm bc} > 5.272\,{\rm GeV/c^2}$ was applied to suppress background. The B signal is described by a Gaussian function with a width fixed from MC. The peak position is fixed to zero if the signal statistical significance is less than 4σ. For decay modes with large numbers of events, the peak position is allowed to float. The background is described by a first-order polynomial, which fits events in the B meson mass sideband $(5.2 < M_{\rm bc} < 5.26)\,{\rm GeV/c^2}$, shown

as the hatched histograms in Fig. 2. The backgrounds under the signals are well reproduced by the B mass sideband events. The fit interval $-0.12 < \Delta E < 0.2\,\mathrm{GeV}$ is chosen to avoid reflections from modes with an additional soft pion, in particular from D^* mesons. The M_{bc} distribution for the range $|\Delta E| < 25\,\mathrm{MeV}$ was fitted by a Gaussian function with a fixed width to describe the signal and by the so-called ARGUS background function [10] with floating exponential and normalization parameters to describe the background. The peak position is fixed to the value $5.2795\,\mathrm{GeV/c^2}$ if the signal statistical significance is less than 4σ. The shape of the background is chosen to be flat if the population outside the signal region is small. The signal yields obtained from the ΔE and M_{bc} fits are listed in Table 2 and found to be in good agreement.

Table 2
The signal yields (obtained from the ΔE and M_{bc} fits), efficiencies (for $K\pi$ and $K\pi\pi\pi$ decay modes), branching fractions, upper limits and significances (the probabilities of a background fluctuation, measured in equivalent σ units) for the studied decay modes. The branching fractions are calculated using the yield from the ΔE fit.

Decay modes	Yield ΔE / M_{bc}	Eff.(%) Kπ/K$\pi\pi\pi$	Br. fractions, upper limits (10^{-4})	Signif. σ
$B^- \to D^0 K^- K^{*0}$	46.7 ± 8.2	7.71	$7.5 \pm 1.3 \pm 1.1$	8.0
	46.4 ± 7.4	-		
$\bar{B}^0 \to D^+ K^- K^{*0}$	87.7 ± 11.4	5.23	$8.8 \pm 1.1 \pm 1.5$	10.4
	88.8 ± 10.2	-		
$B^- \to D^{*0} K^- K^{*0}$	32.8 ± 7.2	2.72	$15.3 \pm 3.1 \pm 2.9$	6.7
	37.3 ± 6.9	0.99		
$\bar{B}^0 \to D^{*+} K^- K^{*0}$	37.5 ± 6.4	3.28	$12.9 \pm 2.2 \pm 2.5$	9.5
	38.6 ± 6.3	1.05		
$B^- \to D^0 K^- K^0$	23.7 ± 5.9	10.25	$5.5 \pm 1.4 \pm 0.8$	5.5
	28.1 ± 5.8	-		
$\bar{B}^0 \to D^+ K^- K^0$	10.3 ± 5.0	6.62	$1.6 \pm 0.8 \pm 0.3$	2.6
	5.8 ± 4.5	-	< 3.1 (90% CL)	
$B^- \to D^{*0} K^- K^0$	9.1 ± 3.9	3.36	$5.2 \pm 2.7 \pm 1.2$	2.5
	10.5 ± 3.5	1.26	< 10.6 (90% CL)	
$\bar{B}^0 \to D^{*+} K^- K^0$	5.4 ± 2.5	4.46	$2.0 \pm 1.5 \pm 0.4$	2.5
	5.6 ± 2.7	1.49	< 4.7 (90% CL)	

Significant signals are observed in the channels with $K^- K^{*0}$ subsystems and in the $B^- \to D^0 K^- K_S^0$ decay mode (Table 2). The signals in the $\bar{B}^0 \to D^+ K^- K_S^0$, $B^- \to D^{*0} K^- K_S^0$ and $\bar{B}^0 \to D^{*+} K^- K_S^0$ decay modes are not statistically significant, and 90% confidence level (CL) upper limits for their

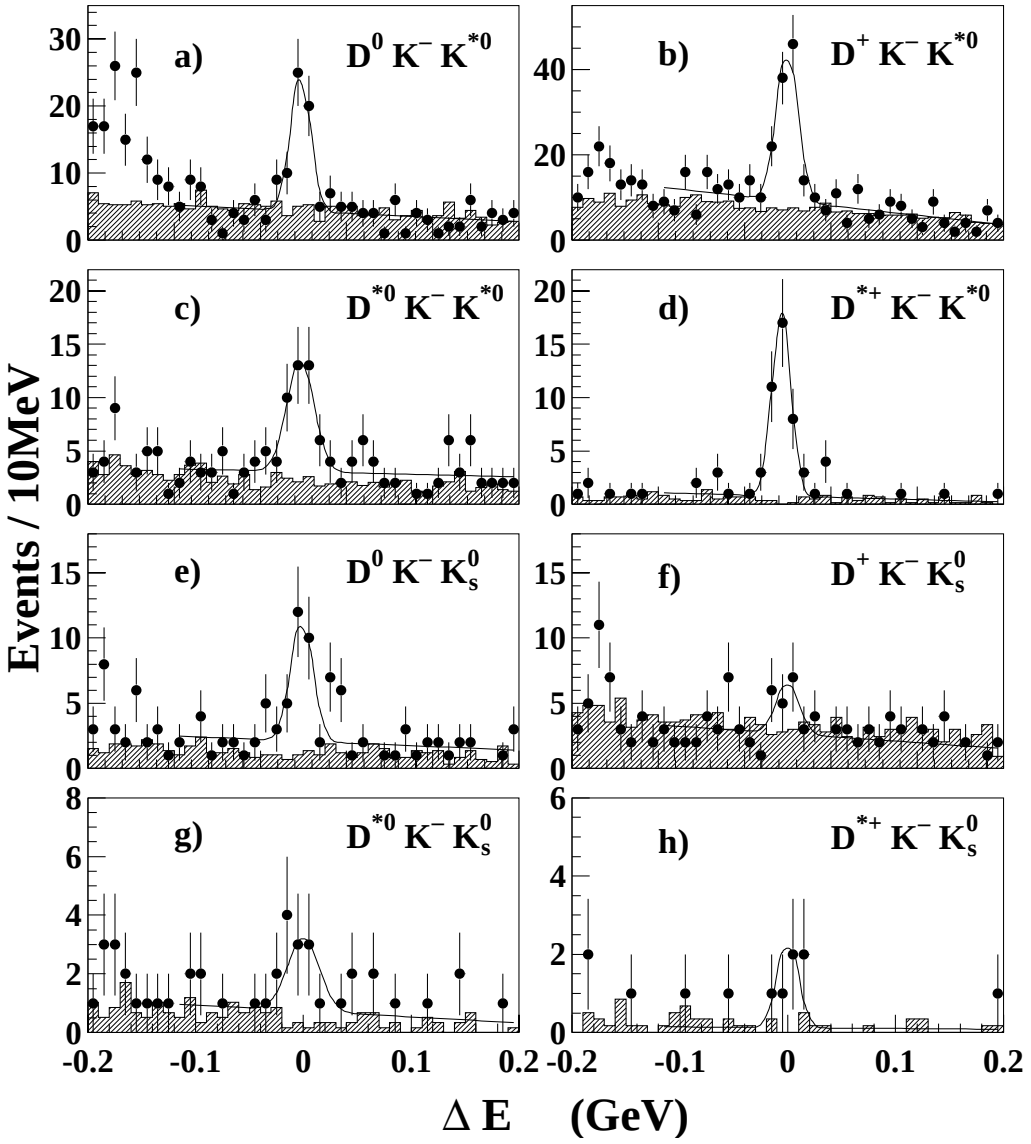

Fig. 2. The ΔE distributions for eight B meson decay channels (see Table 1). The points with error bars are the data, the curves show the results of the fits described in the text. The hatched histogram shows the ΔE distribution for events in the B mass sideband $(5.2 < M_{\rm bc} < 5.26)\,{\rm GeV/c^2}$.

branching fractions are also given in Table 2. We calculate the upper limits assuming a Gaussian distribution of the statistical error, and then inflate the limit by one unit of the systematic error. The branching fractions for the decays of the intermediate D, D^*, K^0 and K^{*0} states were not included in the efficiencies and their values were taken from Ref. [5]. An equal production rate for the neutral and charged B mesons is assumed in the calculation of the branching fractions.

For further analysis the events from the B meson signal region are selected

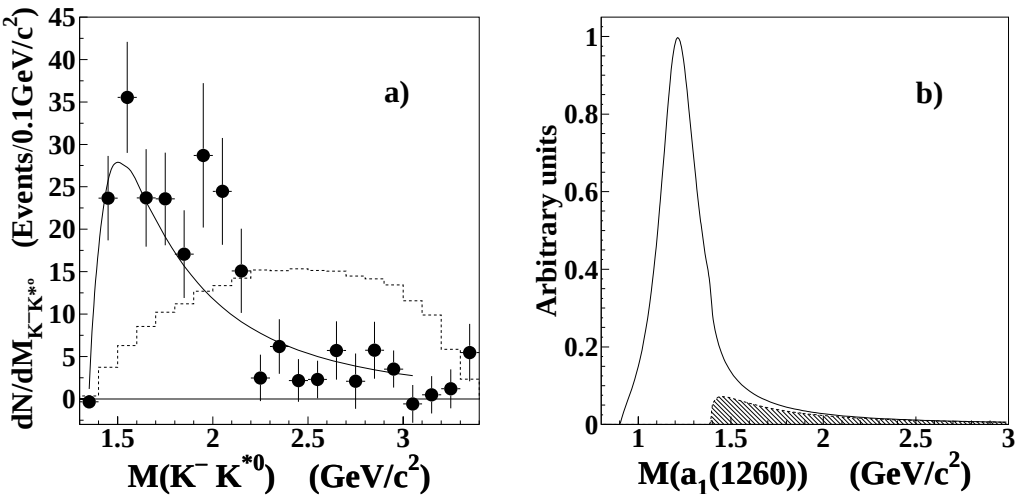

Fig. 3. a) The K^-K^{*0} mass distribution after background subtraction and efficiency correction for the four B decay modes combined. The curve shows the fit to the relativistic Breit-Wigner function described in the text. The dashed histogram shows the distribution for the three-body phase space B decay. b) The shape of the a_1 resonance invariant mass for the $a_1^-(1260) \to \rho^0\pi^-$ decay channel is shown by the solid line. The dashed line (hatched area) shows the shape of the K^-K^{*0} mass distribution for the $a_1^-(1260) \to K^-K^{*0}$ decay channel.

by the requirements $|\Delta E| < 25\,\mathrm{MeV}$ and $M_{\mathrm{bc}} > 5.272\,\mathrm{GeV/c^2}$. The K^-K^{*0} invariant mass distribution after background subtraction and efficiency correction is shown in Fig. 3a for the combined signal region events for the four corresponding B decay modes. The efficiencies as a function of K^-K^{*0} mass are flat within the errors, except for the bin where the D_s^- signal is removed. The background under the B signal is modeled using the M_{bc} sideband.

Simulation of the three-body decay $B \to D^{(*)}K^-K^{*0}$ according to phase space results in the K^-K^{*0} mass distribution shown by the dashed histogram in Fig. 3a. It is clear that the observed shape and an enhancement in the low K^-K^{*0} mass region rule out any significant phase space contribution. A MC simulation assuming an intermediate K^-K^{*0} resonance shows that the observed low mass enhancement can be explained by the quasi-two-body decays $B \to D^{(*)}a_1^-(1260)$, with $a_1^-(1260) \to K^-K^{*0}$. Figure 3b shows the invariant mass of the products of the $a_1^-(1260)$ meson decay via its dominant decay mode $\rho^0\pi^-$ (the solid line) and via the decay mode K^-K^{*0} (the hatched area). The shapes of the distributions were described by relativistic Breit-Wigner functions where both decay channels contribute to the total width simultaneously [11].

The K^-K^{*0} mass distribution was parameterized by the sum of the Breit-Wigner function for a resonance and a phase space function $F_{PS}(M_{KK^*})$ with

a fixed shape for the non-resonant three-body phase space B decay,

$$\frac{dN}{dM_{KK^*}} = \frac{f_{a_1} M_{a_1} \Gamma_{part}(M_{KK^*})}{(M_{a_1}^2 - M_{KK^*}^2)^2 + M_{a_1}^2 \Gamma_{tot}^2(M_{KK^*})} \; + \; f_{PS} \cdot F_{PS}(M_{KK^*}) \quad , (1)$$

where the mass dependence of the partial $\Gamma_{part}(M_{KK^*})$ and total $\Gamma_{tot}(M_{KK^*})$ decay widths is approximated assuming a two-body phase space $a_1 \to KK^*$ decay:

$$\Gamma_{part}(M_{KK^*}) = \Gamma_{KK^*} \cdot (q_{KK^*}/q_0) \; , \qquad \Gamma_{tot}(M_{KK^*}) = \Gamma_{a_1} \cdot (q_{\rho\pi}/q_0). \qquad (2)$$

Here f_{a_1} and f_{PS} are normalization parameters, and M_{a_1} and Γ_{a_1} are the mass and the width of the a_1 resonance. The function $F_{PS}(M_{KK^*})$ describing the three-body phase space distribution obtained by simulation was parameterized by a product of polynomial and threshold functions. The $q_{\rho\pi}$, q_{KK^*} and q_0 parameters are three-vector momenta of each daughter particle in the a_1 rest frame. The constant q_0 is calculated assuming a $a_1 \to \rho\pi$ decay with the mass of the a_1 resonance fixed to its nominal value. The total width $\Gamma_{tot}(M_{KK^*})$ is approximated by the dominant partial width of the $a_1 \to \rho\pi$ decay mode.

If the a_1 mass is fixed to its nominal value $M_{a_1} = 1230\,\mathrm{MeV/c^2}$ [5] and the width is fixed to any value in the range $300 < \Gamma_{a_1} < 600$ MeV/c^2, the relative contribution of the a_1 extracted from the fit is almost 100%. Introducing an additional interference term in the formula (1) leads to a small correction, which does not change the fit results. If the phase space term is omitted, a fit with the resonance width floating gives $\Gamma_{a_1} = (460 \pm 85)\,\mathrm{MeV/c^2}$ (Fig. 3a), which agrees well with the nominal range for the a_1 width [5]. The quality of the fit is reasonable: $\chi^2/n.d.f. = 29.5/18$. Unfortunately, contributions from non-resonant three-body B decays that do not have mass distribution with a phase space shape and/or higher resonances cannot be reliably separated due to the low statistics. The branching fractions for $B \to D^{(*)} a_1^-(1260)$ have been measured by CLEO in the $a_1 \to \rho\pi$ mode [3]. Comparing the CLEO measurement with our results and assuming purely resonant production of the $K^- K^{*0}$ system, the relative fraction $R = Br(a_1^-(1260) \to K^- K^{*0})/Br(a_1^-(1260) \to all)$ is found to be within the range (8-15)% depending on the B decay mode studied. This is larger than the value (3.3 $\pm$ 0.5)% that CLEO obtained by studying the three pion mass shape in τ decays [4].

To study the quantum numbers of the intermediate $K^- K^{*0}$ state, the angular distributions of the final state particles were examined. First, the helicity angle θ_{KK} was defined as the angle between the momentum of the $K^- K^{*0}$ system in the B meson rest frame and the momentum of the K^{*0} in the $K^- K^{*0}$ system rest frame. The helicity angle θ_{K^*}, which was defined as the angle between the momentum of K^{*0} in the $K^- K^{*0}$ system rest frame and the momentum

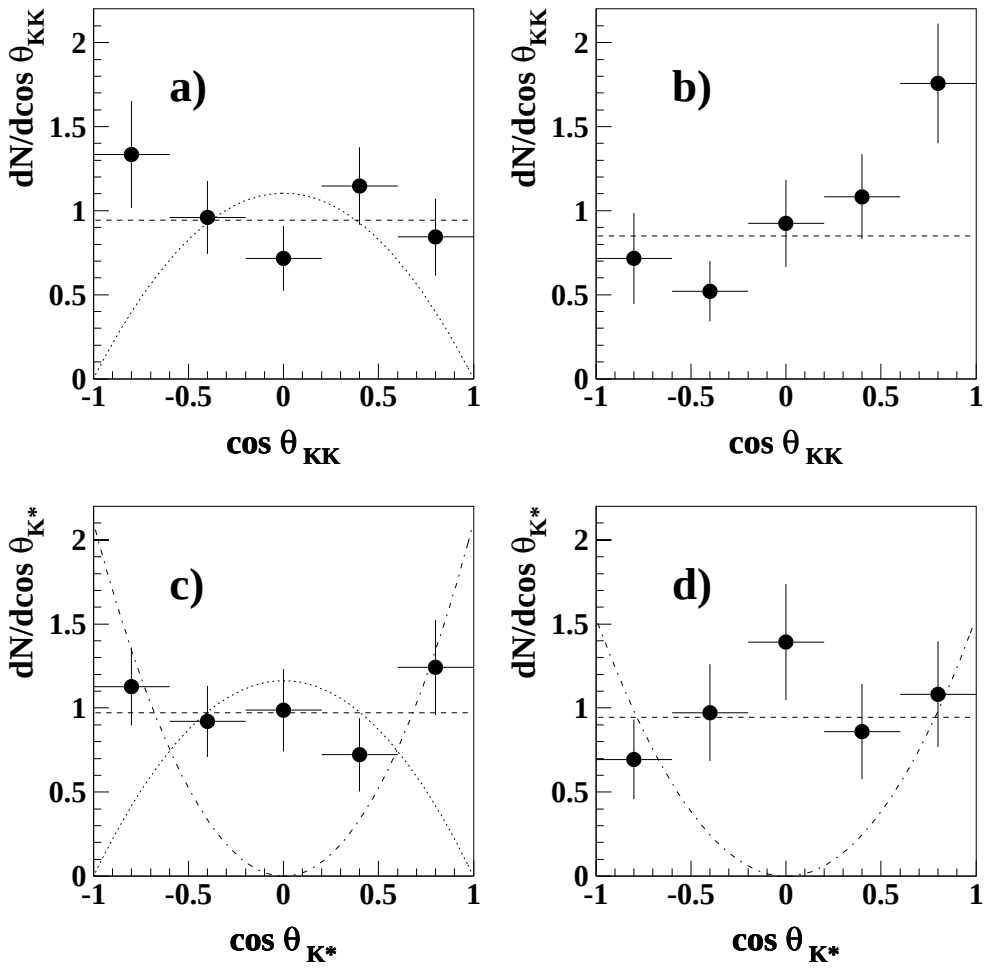

Fig. 4. The $\cos\theta_{KK}$ distributions: a) for the sum of the $B^- \to D^0 K^- K^{*0}$ and $\bar{B}^0 \to D^+ K^- K^{*0}$ modes and b) for the sum of the $B^- \to D^{*0} K^- K^{*0}$ and $\bar{B}^0 \to D^{*+} K^- K^{*0}$ modes. The $\cos\theta_{K^*}$ distributions: c) for the sum of the $B^- \to D^0 K^- K^{*0}$ and $\bar{B}^0 \to D^+ K^- K^{*0}$ modes and d) for the sum of the $B^- \to D^{*0} K^- K^{*0}$ and $\bar{B}^0 \to D^{*+} K^- K^{*0}$ modes. The curves are fits to a constant (dashed), $\sin^2\theta$ (dotted) and $\cos^2\theta$ (dashed-dotted) functions.

of the daughter K^+ meson in the K^{*0} rest frame, was also studied.

Table 3 gives the expected distributions for these two helicity angles for the possible quantum numbers of the $K^- K^{*0}$ system in $B \to D K^- K^{*0}$ and $B \to D^* K^- K^{*0}$ decays. One can see that for $\mathrm{J}^P = 0^-$ and 1^+ the angular distributions for the modes with D and D^* are the same. However, for modes with a D^* and $\mathrm{J}^P = 1^-$ the situation becomes more complicated and the angular distributions depend on the fraction of the longitudinal polarization in the B decay.

Figure 4 shows the $\cos\theta_{KK}$ and $\cos\theta_{K^*}$ distributions for the first four B decay

Table 3
The angular distributions of the K^-K^{*0} system with $J^P = 0^-, 1^-, 1^+$. The values of $\chi^2/n.d.f.$ were obtained from fits to the experimental angular distributions (see Fig. 4).

	D meson modes		D^* meson modes		Sum
J^P	θ_{KK}	θ_{K^*}	θ_{KK}	θ_{K^*}	$\chi^2/n.d.f.$
0^-	const	$\cos^2\theta_{K^*}$	const	$\cos^2\theta_{K^*}$	71.7 / 16
1^-	$\sin^2\theta_{KK}$	$\sin^2\theta_{K^*}$	-	-	37.3 / 8
1^+	const	const	const	const	20.7 / 16

mode combinations after background subtraction and efficiency correction. The angular resolution in these measurements is significantly smaller than the bin size. No significant deviation from the flat dependence is observed for all studied angular distributions, except for the bin at high $\cos\theta_{KK}$ in Fig. 4b. The results of the fits are also shown in Fig. 4. The $\chi^2/n.d.f.$ values given in the last column of Table 3 were obtained by summing the values for the four individual fits. The fit results are consistent with a pure J^P=1^+ state for the K^-K^{*0} system and rule out pure J^P=0^- or J^P=1^- states. It has to be stressed that only decay modes with D mesons are used to test the angular distributions for J^P=1^- case. The fit results support the hypothesis that the intermediate $a_1^-(1260)$ resonant state decays to the K^-K^{*0} final state.

In the four decay modes to $K^-K_S^0$ final states, a clear signal is only observed in the $B^- \to D^0K^-K_S^0$ decay mode (Fig. 2e), the enhancements in the other three decay modes (Figs. 2f,g,h) each have less than 3σ significance. The $K^-K_S^0$ mass spectrum for the $B^- \to D^0K^-K_S^0$ decay mode after background subtraction and efficiency correction is shown in Fig. 5a, where the $D^0 \to K^-\pi^+$ decay channel is used. The mass distribution peaks near the $K^-K_S^0$ mass threshold; the fraction of $B^- \to D^0K^-K_S^0$ signal events in the mass range $M(K^-K_S^0) < 1.3\,\mathrm{GeV/c^2}$ is 55%. The distribution for the three-body phase space B decay is shown by the dashed histogram.

The efficiency corrected and background subtracted helicity angle distribution for the $K^-K_S^0$ system is shown in Fig. 5b. The angle θ_{KK} is defined similarly to that for the K^-K^{*0} system, where the K_S^0 is substituted for the K^{*0}. This distribution is fitted to the form,

$$\frac{dN}{d\cos\theta_{KK}} = A\left(R_L\cos^2\theta_{KK} + (1-R_L)\sin^2\theta_{KK}\right) \quad , \tag{3}$$

where $R_L = \Gamma_L/\Gamma$ is the fraction of longitudinal polarization and A is a free normalization parameter. A fit to the functional form (3) gives the value $R_L = 0.97 \pm 0.08$, which is typical of a P-wave decay of a J^P =1^- system to two pseudoscalar mesons.

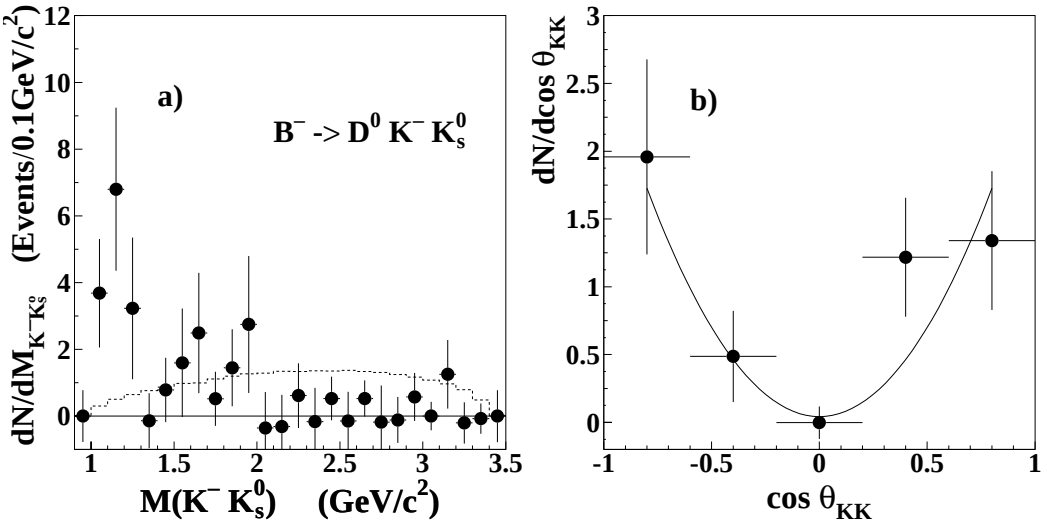

Fig. 5. The fully corrected a) $K^-K^0_S$ invariant mass and b) $K^-K^0_S$ helicity angle distributions. The data are from the $B^- \to D^0K^-K^0_S$ decay mode with $D^0 \to K^-\pi^+$. The dashed histogram shows the expected distribution for three-body phase-space B decays. The curve shows the result of the fit to the function described in the text.

The observed mass distribution is expected to include interfering contributions from the $\rho(770), \rho(1450)$ and $\rho(1700)$ resonances and follow that for the $K\bar{K}$ system produced in the vector isovector state in other processes like e^+e^- annihilation into two kaons or τ^- lepton decays to K^-K^0. Although rather precise measurements of the cross sections exist for the processes $e^+e^- \to K^+K^-$ [12] and $e^+e^- \to K^0_LK^0_S$ [13], the final states observed in e^+e^- annihilation are a mixture of isovector and isoscalar contributions and their separation requires a complicated model-dependent analysis. τ lepton decays are free of this disadvantage since in this case the produced K^-K^0 system always possesses the necessary quantum numbers. CLEO [14] studied this mass distribution in τ decays and concluded that the observed $K^-K^0_S$ mass distribution could qualitatively be described by a ρ-like intermediate mechanism producing an enhancement close to the $K^-K^0_S$ threshold.

The measured branching fractions for the decay modes with the $K^-K^0_S$ system are of the order of $(2-4)\,\%$ relative to those of the respective $B \to D^{(*)}\rho^-(770)$ decay modes with $\rho^-(770) \to \pi^-\pi^0$. These values are at least 5 times larger than one would naïvely estimate, using τ decay branching fractions corrected by phase space factors [15], even taking into account positive interference of the $\rho(770)$ and $\rho(1450)$ resonances.

6 Conclusions

In summary, eight $B \to D^{(*)}K^-K^{(*)0}$ decay modes have been examined for the first time and significant signals have been found for five of them. The branching fractions and upper limits are obtained. Significant signals are observed for the four modes with a K^-K^{*0} system. The K^-K^{*0} mass spectrum is peaked near threshold and smoothly decreases with increasing K^-K^{*0} mass. The angular dependences indicate that the K^-K^{*0} system has $J^P=1^+$. The observed behavior can be interpreted as production of an intermediate $a_1^-(1260)$ resonance that then decays to K^-K^{*0}.

A clear signal is also found in the $B^- \to D^0K^-K_S^0$ decay mode. The $K^-K_S^0$ mass spectrum for this signal is also peaked near the $K^-K_S^0$ mass threshold. The angular dependence shows a $\cos^2\theta_{KK}$ behavior indicating that the $K^-K_S^0$ system has $J^P=1^-$. Some enhancements in the signal regions are also seen in the $B^- \to D^{*0}K^-K_S^0$, $\bar{B}^0 \to D^+K^-K_S^0$ and $\bar{B}^0 \to D^{*+}K^-K_S^0$ decay modes, but with limited statistical significance. A non-resonant three-body contribution, which is not described by phase space, cannot easily be ruled out for any of these decay modes.

7 Acknowledgment

We wish to thank the KEKB accelerator group for the excellent operation of the KEKB accelerator. We acknowledge support from the Ministry of Education, Culture, Sports, Science, and Technology of Japan and the Japan Society for the Promotion of Science; the Australian Research Council and the Australian Department of Industry, Science and Resources; the National Science Foundation of China under contract No. 10175071; the Department of Science and Technology of India; the BK21 program of the Ministry of Education of Korea and the CHEP SRC program of the Korea Science and Engineering Foundation; the Polish State Committee for Scientific Research under contract No. 2P03B 17017; the Ministry of Science and Technology of the Russian Federation; the Ministry of Education, Science and Sport of the Republic of Slovenia; the National Science Council and the Ministry of Education of Taiwan; and the U.S. Department of Energy.

References

[1] M. Bauer, B. Stech and M. Wirbel, Z. Phys. **C34**, 103 (1987).

[2] M. Diehl, *Budapest 2001, High energy physics* hep 2001/104.

[3] CLEO Collaboration, M. S. Alam *et al.*, Phys. Rev. **D50**, 43 (1994).

[4] CLEO Collaboration, D. Asner *et al.*, Phys. Rev. **D61**, 012002 (2000).

[5] Review of Particle Physics, D. E. Groom *et al.*, Eur. Phys. J. **C15**, 1 (2000) and 2001 off-year partial update for the 2002 edition available at http://pdg.lbl.gov.

[6] R. Aleksan *et al.*, Phys. Rev. **D62**, 093017 (2000).

[7] E. Kikutani ed., KEKB Accelerator Papers, KEK Preprint 2001-157 (to be published in Nucl.Inst. and Meth. A).

[8] Belle Collaboration, A. Abashian *et al.*, Nucl. Instr. Meth. **A479**, 117 (2002).

[9] G. C. Fox and S. Wolfram, Phys. Rev. Lett. **41**, 1581 (1978).

[10] ARGUS Collaboration, H. Albrecht *et al.*, Phys. Lett. **B229**, 304 (1989).

[11] J. D. Jackson, Nuovo Cim. **34**, 1644 (1964).

[12] B. Delcourt *et al.*, Phys. Lett. **B99**, 257 (1981); P. M. Ivanov *et al.*, Phys. Lett. **B107**, 297 (1981); D. Bisello *et al.*, Z. Phys. **C39**, 13 (1988).

[13] F. Mané *et al.*, Phys. Lett. **B99**, 261 (1981); P. M. Ivanov *et al.*, JETP Lett. **36**, 112 (1982).

[14] CLEO Collaboration, T. E. Coan *et al.*, Phys. Rev. **D53**, 6037 (1996).

[15] F. J. Gilman and D. H. Miller, Phys. Rev. **D17**, 1864 (1978); N. Kawamoto and A. I. Sanda, Phys. Lett. **B76**, 446 (1978); K. K. Gan, Phys. Rev. **D37**, 3334 (1988).